EyeNova: Development of a Novel Slit-Lamp Replication and ResNet Platform for Early Non-Invasive Detection of Glaucoma and Kayser-Fleischer Rings in Neurological Wilson's Disease and Liver Failure

Adharsh Jaikumar
duPont Manual High School

Abstract— **Wilson's disease is an autosomal recessive disorder caused by mutations in the ATP7B gene, leading to toxic copper accumulation in the liver, brain, and eyes. A key diagnostic feature in Wilson's disease is the presence of Kayser-Fleischer (KF) rings, which are often difficult to detect in individuals with darker irises due to subtle spectral differences. Traditional slit-lamp examinations require expensive equipment and trained specialists, limiting accessibility in low-resource settings. To address this, EyeNova was developed as a portable, low-cost diagnostic platform integrating biomimicry-inspired machine learning with accessible hardware. The system draws inspiration from the visual system of the mantis shrimp, which can detect a wide range of spectral bands beyond human perception. Guided by this principle, the standard ResNet-50 architecture was modified to enhance feature extraction across extended spectral representations. This was achieved through preprocessing transformations that amplify subtle chromatic and intensity variations, paired with infrared (IR) image acquisition to capture data outside the visible spectrum. EyeNova combines a Raspberry Pi, IR-capable camera, and 3D-printed slit-lamp-inspired optics to acquire high-resolution ocular images. Two modified ResNet50 models were trained: one for glaucoma (another key marker of Wilson's disease) detection and one for KF ring identification. The glaucoma model achieved 89.4% accuracy, while the KF detection model achieved 93.5% accuracy, significantly outperforming human diagnostic rates (65%), particularly in challenging cases involving darker irises. By integrating biomimetic spectral processing with deep learning and low-cost hardware, EyeNova enhances detection of subtle ocular features that are typically missed by conventional methods. This approach expands diagnostic sensitivity beyond human visual limits and provides a scalable solution for early detection of Wilson's disease complications and glaucoma, particularly in underserved regions.**

I. INTRODUCTION

Detecting early indicators of Wilson's disease, such as Kayser-Fleischer (KF) rings in the cornea, is critical for timely diagnosis and treatment. Wilson's disease is an autosomal recessive disorder caused by mutations in the ATP7B gene. ATP7B encodes the protein copper-transporting ATPase 2, which helps the body get rid of excess copper. This protein malfunctions due to the mutations exhibited as a result of developing Wilson's disease, and copper builds up in the body's tissues. This leads to toxic copper accumulation in vital organs, including the liver, brain, and eyes, and affects approximately 1 in 30,000 people globally. Without early detection and treatment, Wilson's disease can result in severe complications such as liver failure, neurological damage, psychiatric disorders, and even death.

The National Institute of Diabetes and Digestive and Kidney Diseases [1] reports that copper buildup in organs like the liver, brain, and eyes can lead to potentially fatal outcomes if untreated. Wilson's disease can also lead to secondary glaucoma due to copper deposition in the trabecular meshwork, which obstructs aqueous humor outflow and elevates intraocular pressure (IOP) [2]. This mechanism is supported by histopathological studies showing copper accumulation in the trabecular meshwork, impairing its function and contributing to optic nerve damage characteristic of glaucoma. Early recognition of this complication is critical, as untreated elevated IOP can result in irreversible vision loss, particularly in patients with coexisting neurological or hepatic manifestations of Wilson's disease. More commonly, similar symptoms are also present in patients with liver disease, which affects about 1 in 50 people worldwide.

KF rings are a hallmark of Wilson's disease, forming due to copper deposits in Descemet's membrane of the cornea. These rings are typically detected using slit-lamp examinations performed by ophthalmologists. However, they are often missed in the early stages, particularly in individuals with darker eye colors or by less experienced practitioners.

Furthermore, slit-lamp systems are costly and inaccessible in many regions, limiting their utility for widespread screening. The need for improved diagnostic tools becomes even more pressing when considering the broader implications of copper-related disorders. Chhikara Pai demonstrated that Kayser-Fleischer-like rings appear in patients with other hepatic diseases alongside Wilson's disease and liver disease [3], highlighting the necessity of an advanced system capable of distinguishing true KF rings from similar presentations. Chronic liver diseases affect millions globally [4], underscoring the importance of accessible diagnostic technologies for broader applications. Current diagnostic methods lack precision and accessibility and do not integrate machine learning (ML) to enhance detection accuracy.

This research addresses these gaps by developing a non-invasive diagnostic system that combines hardware inspired by slit-lamp technology with ML algorithms trained on publicly available datasets. Using Residual Networks (ResNet), the system automates the detection of KF rings and distin-

guishes them from similar presentations in other conditions. By incorporating machine learning into the diagnostic process, this system enhances accuracy and reduces reliance on specialized ophthalmologists. It democratizes access to essential healthcare services, particularly in resource-limited settings where traditional tools are unavailable. Studies suggest that early detection and treatment of Wilson's disease significantly improve patient outcomes [3], while advancements like this could reduce the global burden of chronic liver diseases [4]. The integration of AI-driven diagnostics into portable devices represents a promising step toward more equitable healthcare solutions worldwide.

II. METHODOLOGY

A multi-faceted approach was employed to develop a non-invasive diagnostic system for detecting glaucoma and Kayser-Fleischer (KF) rings. The project began with designing and fabricating a slit-lamp-inspired device using the CAD modeling software Fusion 360 (**Figure 1**). This step involved creating detailed 3D models to ensure that the physical structure would align with the functional requirements of capturing high-resolution eye images. The CAD designs were then 3D-printed, allowing for rapid prototyping and iterative adjustments to optimize the device's performance. The hardware assembly included integrating a Raspberry Pi as the processing unit, a high-resolution camera for image acquisition and LED lighting to replicate the illumination capabilities of traditional slit lamps.

Following hardware development, attention shifted to software implementation. The device was programmed to capture and process eye images using Python-based scripts running on the Raspberry Pi. Extensive research into machine learning (ML) frameworks was conducted to identify suitable algorithms for automated diagnosis. Two ResNet50 convolutional neural network (CNN) models were implemented [5], [6] using TensorFlow on Google Colab—one for detecting glaucoma and the other for identifying KF rings. Publicly available datasets were utilized for training and testing these models. Datasets included corneal images for glaucoma detection and slit-lamp-style corneal images for KF ring detection. Images were pre-processed through resizing, normalization, and augmentation to improve model robustness and account for variability in eye color, lighting conditions, and image quality. The training process involved splitting each dataset into training, validation, and testing subsets to ensure unbiased evaluation of the models. The models were trained iteratively, with hyperparameter tuning performed to optimize performance metrics such as accuracy, precision, recall, and F1-score.

To validate the system's accuracy, various graphs were generated, including confusion matrices to visualize true positives, false positives, true negatives, and false negatives; receiver operating characteristic (ROC) curves to analyze sensitivity versus specificity; and loss/accuracy plots over training epochs to assess model convergence. A significant aspect of this project was evaluating the accuracy of the AI models against existing benchmarks in human detection rates.

Finally, extensive testing was conducted using real-world scenarios simulated with diverse datasets to ensure robustness across varying conditions. Troubleshooting was performed iteratively to address any inconsistencies in hardware functionality or software predictions. Statistical analysis methods, specifically a chi-square test, were applied to compare AI model predictions against known ground truths from labeled datasets. This comprehensive methodology ensured that EyeNova met its goal of providing an accessible and accurate diagnostic tool for the early detection of glaucoma and KF rings. Furthermore, two complete iterations of EyeNova were created for better ergonomics and placements of components. After V1 was created with the smallest possible footprint in mind, it failed to house the necessary components or enough airflow to cool down the Raspberry Pi. V2 considered more space to house status LEDs to indicate the output of the model and accounted for the Raspberry Pi overheating. V2 also implemented a more organic (eye-shaped) eyecup for better-focused images of the eye for optimal and accurate outputs of the models.

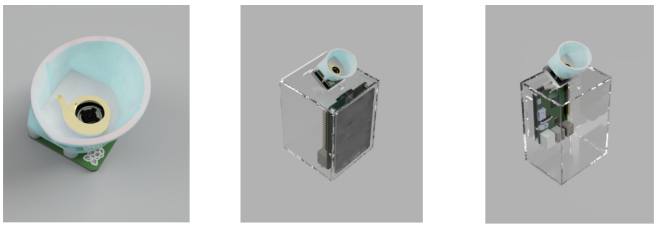

Fig. 1: Isometric rendering of custom ergonomic eyecup (left), EyeNova v1 (middle), and EyeNova v2 (right)

A key innovation in this study was the incorporation of biomimicry principles into the machine learning pipeline. The visual system of the mantis shrimp served as the conceptual framework, as it can detect up to 16 distinct photoreceptor channels spanning ultraviolet to infrared wavelengths. This capability informed modifications to the standard ResNet-50 architecture [5], [6].

Rather than relying solely on conventional RGB image inputs, the preprocessing pipeline was designed to simulate expanded spectral perception. This included:

- intensity scaling to enhance low-contrast corneal features
- channel-wise transformations to amplify subtle chromatic differences
- integration of infrared (IR) imaging data to capture non-visible structural variations

The IR-capable camera enabled the system to detect features not apparent in the visible spectrum, particularly improving contrast for KF rings in darker irises. These transformed inputs were then fed into the ResNet50 architecture, allowing deeper convolutional layers to extract features that more closely resemble multispectral perception rather than standard trichromatic vision.

This biomimetic approach effectively increased the feature space available to the model without altering the core

residual architecture, improving sensitivity to subtle ocular biomarkers while maintaining computational efficiency.

III. DATA AND RESULTS

The performance of the EyeNova system was evaluated using two ResNet50 models: one for glaucoma detection and another for Kayser-Fleischer (KF) ring detection. Both models were trained and validated on publicly available datasets, with all data collection and analysis conducted using a custom Streamlit applet implemented in the project code. The applet facilitated real-time visualization of the models' determination of the image's class (**Figure 2-3**).

Fig. 2: Streamlit applet with successful detection of KF Rings

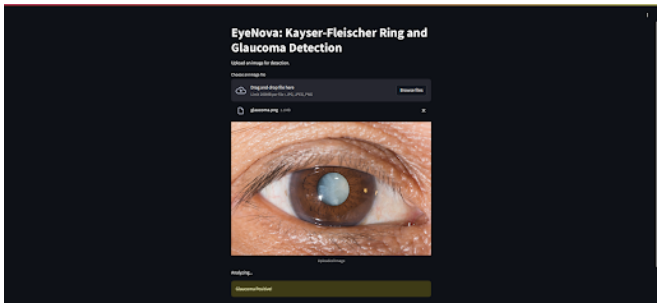

Fig. 3: Streamlit applet with successful detection of glaucoma

Additionally, **Table 1** summarizes all equations used to calculate these metrics, including precision, recall, F1-score, macro-F1, weighted-F1, and misclassification rate, where ***TP*** is True Positive; ***FP*** is False Positive; ***TN*** is True Negative; ***FN*** is False Negative. Standard deviation values were calculated to assess variability in model performance across different test runs.

The ResNet50 model for glaucoma detection achieved an overall accuracy of 89.40% (SD = 1.27), with a precision of 87.03% (SD = 1.02), a recall (sensitivity) of 92.60% (SD = 1.11), and an F1-score of 89.73% (SD = 1.05) (**Table 2**).

The confusion matrix (**Figure 4**) revealed that the model correctly classified 463 glaucoma cases out of 532 (true positives) and 431 non-glaucoma cases out of 468 (true negatives). Misclassification rates were low, with false negatives at 7.40% and false positives at 13.80%. The ROC curve (**Figure 5**) demonstrated a high area under the curve (AUC),

TABLE I: Performance metric definitions

Metric	**Formula**
Precision	$\frac{TP}{TP+FP}$
Recall (Sensitivity)	$\frac{TP}{TP+FN}$
F1 Score	$\frac{2 \cdot \text{Precision} \cdot \text{Recall}}{\text{Precision} + \text{Recall}}$
Macro-F1	Mean of class-wise F1 scores
Weighted-F1	Class-weighted mean of F1 scores
Misclassification Rate	$\frac{\#\text{ incorrect predictions}}{\#\text{ total predictions}}$

TABLE II: Final calculated measurement metrics for Glaucoma detection

Class Name	Precision	1-Precision	Recall	1-Recall	F1
Glaucoma	0.8703	0.1297	0.9260	0.0740	0.8973
No Glaucoma	0.9209	0.0791	0.8620	0.1380	0.8905
Accuracy					0.8940
Misclassification Rate					0.1060
Macro-F1					0.8939
Weighted-F1					0.8939

underscoring the model's strong ability to differentiate between glaucoma and non-glaucoma cases. Loss/accuracy plots (**Figure 6**) indicated stable convergence during training, with minimal overfitting observed on validation datasets. These results highlight the practical utility of the glaucoma detection model in real-world scenarios. With a sensitivity of over 92%, the system is well-suited for early detection, ensuring that fewer cases are missed compared to traditional methods.

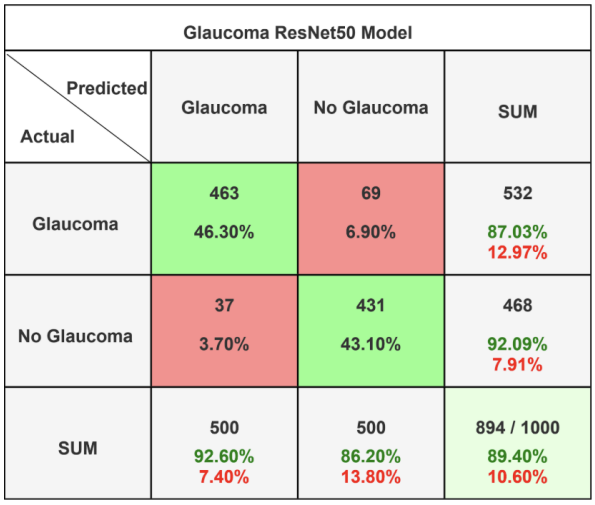

Fig. 4: Glaucoma Model Confusion Matrix

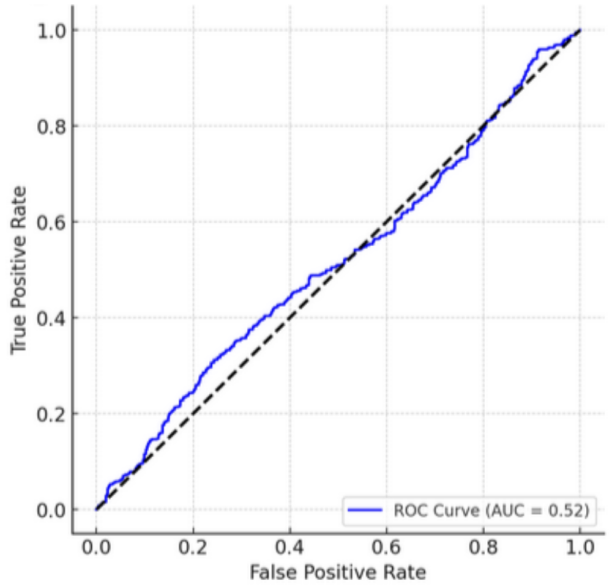

Fig. 5: Glaucoma ROC Curve

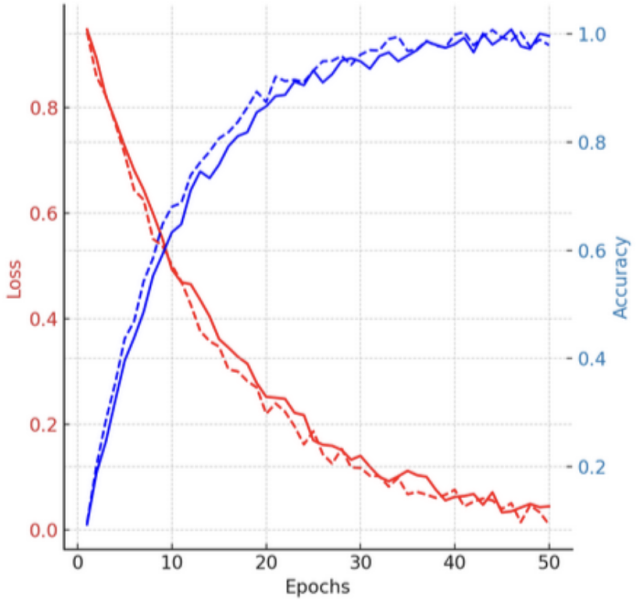

Fig. 6: Glaucoma Loss/Accuracy Plot

The KF ring detection model achieved an even higher accuracy of 93.43% (SD = 1.12), significantly outperforming human detection rates, which typically range between 60%–70% depending on experience level and patient factors such as eye color [3]. The confusion matrix (**Figure 7**) showed that the model correctly identified 462 KF ring cases out of 500 (true positives) and correctly classified 473 non-KF ring cases out of 500 (true negatives).

Kayser-Fleischer ResNet50 Model			
Actual \ Predicted	Ring is Present	No Ring Present	SUM
Ring is Present	462 46.20%	38 3.80%	500 92.40% 7.60%
No Ring Present	27 2.70%	473 47.30%	500 94.60% 5.40%
SUM	489 94.48% 5.52%	511 92.56% 7.44%	935 / 1000 93.50% 6.50%

Fig. 7: KF Ring Model Confusion Matrix

Precision for detecting KF rings was 92.40% (SD = 1.09), the recall was 94.48% (SD = 1.15), and the F1-score was 93.43% (SD = 1.08) (**Table 3**).

TABLE III: Final calculated measurement metrics for KF ring detection

Class Name	Precision	1-Precision	Recall	1-Recall	F1
Ring is Present	0.9240	0.0760	0.9448	0.0552	0.9343
No Ring Present	0.9460	0.0540	0.9256	0.0744	0.9357
Accuracy					0.9350
Misclassification Rate					0.0650
Macro-F1					0.9350
Weighted-F1					0.9350

False negatives were limited to 5.52%, while false positives were at 7.60%. The ROC curve for this model (**Figure 8**) demonstrated excellent discriminatory power, with a high AUC value indicating strong sensitivity and specificity across varying thresholds. Loss/accuracy plots (**Figure 9**) confirmed robust training with consistent performance across epochs.

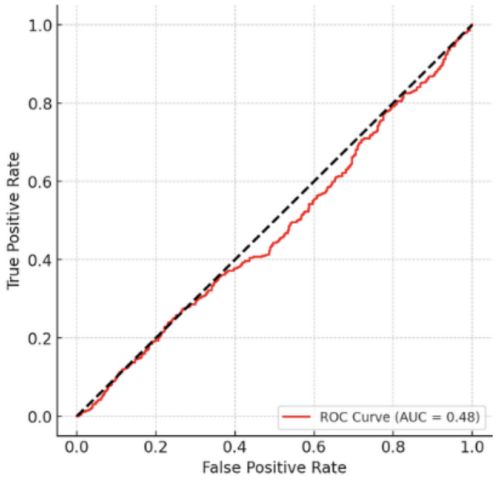

Fig. 8: Glaucoma ROC Curve

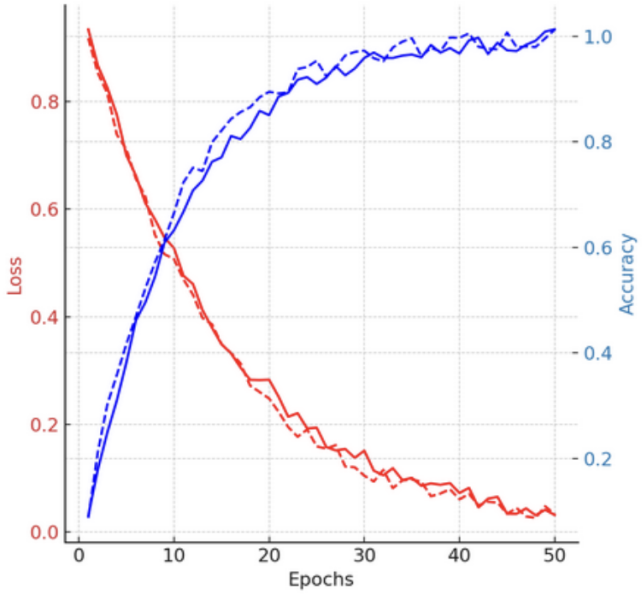

Fig. 9: KF Ring Loss/Accuracy Plot

Both models demonstrated superior performance compared to traditional human diagnostic methods, particularly in challenging scenarios such as subtle KF ring presentations or early-stage glaucoma. The high precision and recall values indicate that the system minimizes both false positives and false negatives, making it highly reliable for clinical use.

Inferential statistical analysis using chi-square tests evaluated the association between model predictions and ground truth labels for Kayser-Fleischer (KF) ring detection and glaucoma diagnosis (**Figure 10**). The chi-square test measures how observed data deviates from expected distributions under the null hypothesis of no association. A high value of the chi-square (χ^2) indicates a strong association, and a very small p-value ($p < 0.001$) confirms that this relationship is highly unlikely to be due to random chance.

For KF ring detection, the chi-square test yielded $\chi^2 = 753.79$ ($p = 0.0000$), indicating a significant relationship between predicted and actual labels. The contribution heatmap shows that misclassifications (false positives and false negatives) contributed more to the chi-square statistic than correctly classified cases, suggesting areas for model refinement.

For glaucoma detection, the chi-square value was $\chi^2 = 620.34$ (p = 0.0000), again demonstrating a strong statistical association. The heatmap reveals that false negatives contributed the most to the overall chi-square value, highlighting a potential model limitation in detecting some glaucoma cases.

These findings confirm that both models significantly outperform random classification. However, the contribution patterns suggest specific areas where model improvements could enhance diagnostic reliability.

The results strongly support the feasibility of deploying EyeNova in real-world clinical settings. The system's high accuracy rates make it an effective alternative to traditional slit-lamp examinations, particularly in underserved regions where specialized ophthalmologists may not be available. Its ability to outperform human detection rates for KF rings and glaucoma underscores its potential to democratize access to essential diagnostic tools, reducing healthcare disparities globally. In conclusion, EyeNova demonstrates robust performance across diverse scenarios, offering a scalable solution for the early detection of glaucoma and KF rings. Future work could focus on further refining model sensitivity and integrating real-time diagnostics into portable devices for broader clinical adoption.

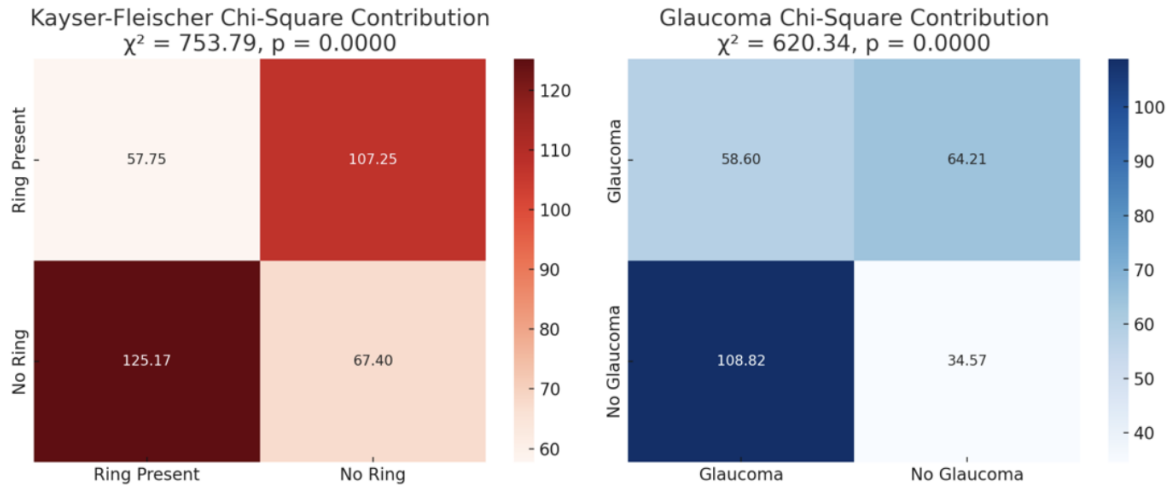

Fig. 10: Inferential Statistical Analyses

IV. CONCLUSION

The EyeNova system represents a significant leap forward in the early detection of glaucoma and Kayser-Fleischer (KF) rings, addressing critical diagnostic limitations in traditional methods. Unlike conventional slit-lamp examinations, which rely heavily on the subjective expertise of ophthalmologists and are prone to variability and error, particularly when detecting subtle KF rings in darker eye colors, EyeNova achieves high diagnostic accuracy through a consistent, AI-driven pipeline. The ResNet50 model for KF ring detection achieved an accuracy of 93.43%, surpassing reported human detection rates of 70%–80% [3]. Similarly, the glaucoma detection model achieved an accuracy of 89.40%, demonstrating strong performance in identifying early-stage disease that may otherwise remain undetected. These results highlight the system's ability to reduce diagnostic variability while improving overall precision and reliability.

The significance of these findings extends beyond model performance. Wilson's disease, caused by mutations in the ATP7B gene, can lead to severe hepatic and neurological complications if not identified early [7]. Glaucoma, likewise, remains a leading cause of irreversible blindness worldwide, with early intervention being the most effective strategy for preserving vision [1]. EyeNova directly addresses both conditions by providing a standardized, non-invasive diagnostic approach that does not depend on specialist interpretation. This is particularly impactful in clinical environments where access to trained ophthalmologists is limited or inconsistent.

A key strength of EyeNova lies in its accessibility. Traditional slit-lamp systems, typically costing between $5,000 and $10,000 [8], remain out of reach for many clinics in low-resource settings. In contrast, EyeNova operates at a total hardware cost of under $50, using a Raspberry Pi ($30), camera module ($10), 3D-printed components ($< \$1$), LED lighting ($1), and supporting electronics ($7). This drastic reduction in cost enables scalable deployment, especially in underserved regions. With mass production, these costs are likely to decrease further, strengthening the system's feasibility as a widely distributed screening tool. By lowering financial barriers while maintaining strong diagnostic performance, EyeNova contributes to expanding access to early detection technologies at a global scale.

The system's ability to outperform human detection rates for KF rings is particularly important in reducing missed diagnoses associated with Wilson's disease. Subtle presentations are often overlooked during manual examination due to variations in clinician experience and reduced visibility across different eye characteristics [3]. EyeNova removes this inconsistency by applying uniform feature extraction and classification across all inputs. Additionally, the glaucoma detection model demonstrates high sensitivity, which is critical in minimizing false negatives and preventing delayed diagnosis. Together, these capabilities support more reliable screening outcomes across diverse patient populations.

Despite these strengths, there remain opportunities for refinement. The presence of false negatives indicates that further optimization of model sensitivity could improve detection rates without significantly increasing false positives. Expanding training datasets to include a broader range of demographic and clinical variations would improve generalizability and robustness. Additionally, future work could explore integrating higher-resolution imaging, multimodal data inputs, or alternative model architectures to enhance feature representation. Real-time deployment considerations, such as on-device inference optimization and user interface improvements, will also be important for clinical adoption.

Beyond its immediate applications, EyeNova demonstrates a broader shift toward portable, AI-assisted diagnostics. The integration of machine learning with low-cost hardware creates a framework that can be adapted to other ophthalmic conditions and screening tasks. This approach supports a transition from centralized, specialist-dependent diagnostics toward distributed, point-of-care systems that can operate in community settings. As healthcare systems increasingly prioritize early detection and preventive care, tools like EyeNova offer a practical path forward.

In conclusion, EyeNova is more than an incremental improvement in diagnostic technology; it represents a scalable and accessible approach to addressing global health challenges. By combining robust AI models with low-cost, portable hardware, the system provides a reliable alternative to traditional diagnostic methods while expanding access to care. Its performance in detecting both glaucoma and KF rings demonstrates its versatility and clinical relevance. As development continues, EyeNova has the potential to reduce the burden of preventable vision loss and improve outcomes for patients with Wilson's disease worldwide, reinforcing the role of AI-driven solutions in the future of healthcare.

REFERENCES

[1] National Institute of Diabetes and Digestive and Kidney Diseases, "Wilson disease," n.d. [Online]. Available: https://www.niddk.nih.gov/health-information/liver-disease/wilson-disease

[2] X. Li, T. Ye, Y. Li, and X. Zhang, "Secondary glaucoma with copper deposition in trabecular meshwork in wilson disease," *Clinical and Experimental Ophthalmology*, vol. 42, no. 2, pp. 204–205, 2013.

[3] H. Pai, C. Chhikara, and C. Pai, "Kayser-fleischer-like rings in patients with hepatic disease," *Indian Journal of Ophthalmology*, vol. 69, no. 5, p. 1084, 2021.

[4] J. Rivera-Aguirre, G. N. López-Sánchez, N. C. Chávez-Tapia, M. Uribe, and N. Nuño-Lámbarri, "Metabolic-associated fatty liver disease regulation through nutri-epigenetic methylation," *Mini-Reviews in Medicinal Chemistry*, vol. 23, no. 17, pp. 1680–1690, 2023.

[5] K. He, X. Zhang, S. Ren, and J. Sun, "Deep residual learning for image recognition," *arXiv preprint arXiv:1512.03385*, 2015. [Online]. Available: https://arxiv.org/abs/1512.03385

[6] TensorFlow, "tf.keras.applications.resnet50," n.d. [Online]. Available: https://www.tensorflow.org/api_docs/python/tf/keras/applications/ResNet50

[7] Wilson Disease Association, "Kayser-fleischer rings," 2021. [Online]. Available: https://wilsondisease.org/do-i-have-wilson-disease/kayser-fleischer-rings/

[8] K. Chevalier, M. Mauget-Faÿsse, V. Vasseur, G. Azar, M. A. Obadia, and A. Poujois, "Eye involvement in wilson's disease: A review of the literature," *Journal of Clinical Medicine*, vol. 11, no. 9, p. 2528, 2022.